2005-01-3510

Edge-Seal Mounting Support for Diesel Particulate Filters

Sivanandi Rajadurai, Shiju Jacob, Chad Serrell, Rob Morin, Zlatomir Kircanski, and Mike McCarthy

ACS Industries Inc.

ABSTRACT

Due to the large sizes, high bulk densities and high thermal expansion coefficients of diesel particulate filter (DPF) substrates, conventional mounting systems fail to provide sufficient mounting pressures. L-Seal mounting supports used in DPF applications not only provide these forces but also cushion the system, accommodating linear tolerance variations in the cone, shell and substrate. The mounting forces provided can be altered by changing various aspects of the seal itself including the material used, its surface characteristics, any heat-treatment applied and its wire geometry. Cyclical compression tests show proportional increases in compressive force per unit of weight, indicating a dimensional consistency in the L-Seal design. The compression characteristics of A286 increase significantly (>20%) during heat treatment as the material precipitate work-hardens. Further heat treatment at DPF regeneration temperatures does not alter the compression characteristics of the material. Combining A286 with a traditional 310 SS allows for generation of optimal spring-back rates otherwise unattained by using than an all 310 or A286 material. The combination stabilizes during cyclic testing, retaining a residual force of more than 50% of its initial value. Within the elastic limits of the L-Seal, the relative loss of force during these tests as a function of the closing gap is constant.

INTRODUCTION

Particulate filters have proven to be highly effective cleaning up diesel exhausts [1-3]. Starting in 2007, DPF usage will be required as particulate matter must be reduced from 0.10 g/bhp-h to 0.01g/bhp-h as measured by the U.S. Heavy-Duty FTP transient cycle [1, 4]. Different filter substrate materials such as advanced ceramics, SiC, knitted ceramic and various metals [5-7] have been selected based on their high filter efficiency, thermal shock

resistance, low space requirements, low system mass and low thermal expansion coefficients [8]. Support rings, edge pins and cone modifications assist in retaining and providing axial support to the substrate. These modifications, however, tend to affect the linear tolerance of the substrate (+/-2 mm). A wire mesh, L-shaped edge seal (L-Seal) provides a cushion, accommodating the different converter components' linear tolerance variations as well as providing the necessary axial and radial mounting pressures needed to hold the substrate in place.

DIESEL PARTICULATE FILTERS

The DPF is different [9] from the more common ceramic catalytic converter substrates because of its checkerboard, alternate cell opening construction. Exhaust gas enters the filter upstream through an open cell and is forced through the porous cell walls when it encounters the closed, downstream end of the channel. Since the particulate matter is larger than the pore size of the cell walls, it is trapped as the exhaust gas passes through. This type of filtration, also known as the Wall Flow Concept, provides a large filter surface area within a compact volume.

The substrate is a honeycomb structure, extruded from a porous ceramic cordierite or silicon carbide. Crystallized SiC has been used since 2000, when it was identified as a means of solving the PM-NOx trade-off problem. SiC is one of the hardest materials known to man and has unique physical attributes which allow it to handle thermal regeneration and provide this level of filtration capability [5]. Table 1 compares the physical attributes of Cordierite and SiC.

Material	Cordierite	SiC
Melting Point (^{o}C)	1460	2400
Cell density (cpsi)	178	185
Wall thickness (mil)	12	18
Bulk density (g/cc)	0.45	0.85
Porosity %	50	43
Thermal Conductivity (W/m K)	<2	20
Specific Heat (J/g ^{o}C)	1.11	1.12
Coeff. Of thermal expansion CTE (µm/m ^{o}C)	0.7	4.4
Elastic modulus eMod (GPa)	4.7	33.3
Modulus of Rupture MOR (MPa)	2.6	18.3
Thermal Shock Parameter TSP=MOR/CTE x eMod (^{o}C)	790	125

Table 1: Cordierite and SiC physical attributes

While cordierite exhibits a low thermal expansion coefficient and is able to survive thermal shock, it is limited by its low heat capacity and is susceptible to ash reaction at high temperatures. Sic, on the other hand, offers low thermal shock resistance and a high thermal expansion coefficient. It also needs to be segmented in order to protect it from on-road mechanical or DPF regeneration induced thermal shocks [8]. The segmentation process

can increase potential mechanical integrity issues.

When a DPF is in use, particulate loading increases backpressure and which affects the axial force exerted on the substrate. The mounting system selected needs to handle this force as well as that exerted by thermal, mechanical and road-load conditions. A properly designed L-Seal provides more than enough axial and radial support. The thermal spike absorbed during DPF regeneration requires an appropriate insulation be used with L-Seal supports in order to maintain the necessary external shell skin temperature.

L-SEAL

An L-Seal is simply an “L” shaped edge seal made from knitted wire mesh. It provides radial and axial support to the substrate. Figure 1 shows the L-Seal design dimensions.

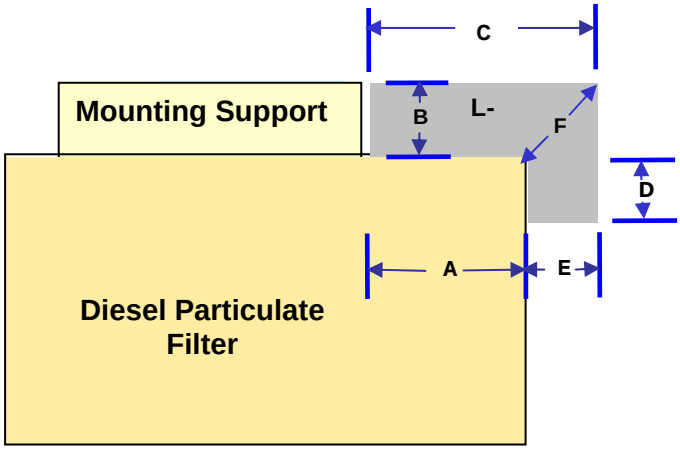

A = LEG LENGTH
B = RADIAL GAP
C = OVERALL LEG LENGTH
D = AXIAL WIDTH
E = AXIAL HEIGHT
F = DIAGONAL WIDTH

Figure 1: L-Seal Design Dimensions

Wire mesh compression characteristics can vary depending on the material used, its surface profile, surface characteristics, strands per knit, temper, thermal impacts, geometries and the density of the pressed seal.

MOUNTING FORCE

Figure 2 illustrates forces exerted on a DPF during actual use.

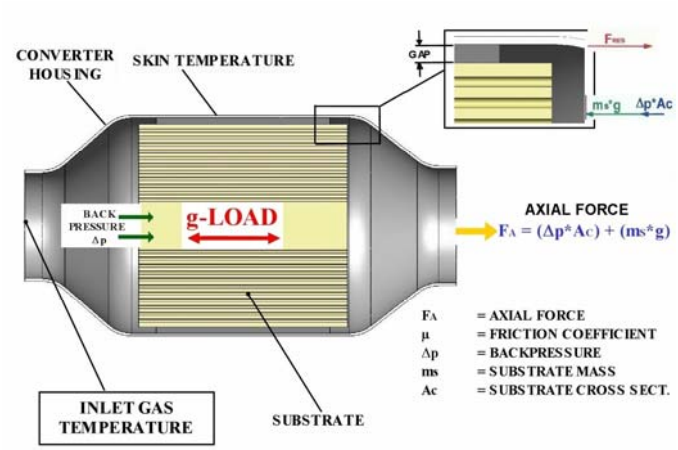

Figure 2: Forces Exerted on a DPF

AXIAL FORCE

The axial force required to hold the substrate in place depends on the mass of the substrate, the acceleration load, the backpressure and the substrate’s frontal surface area and is a function of backpressure and inertial force.

Axial Force (F_A) = Backpressure Force (F_B) + Inertial Force (F_I)

$F_A = (\Delta p \times A_C) + (m_s \times a)$

Table 2 shows the axial force exerted, g-load and backpressure for different substrate materials and masses.

Attributes	SiC		Cordierite	
Substrate (D x L), in	10.5 x 12	13 x 17	10.5 x 12	13 x 17
Substrate Mass, kg	15.5	33.6	9.5	20.7
G load, g	20	40	20	40
Back pressure, kPa	40	80	40	80
Axial force, kN	5.5	20	4.1	15

Table 2: Forces Exerted on Substrates

Ideally, a support system will provide enough axial and radial compensating force so that either one or both can effectively hold the system. This also accounts for any deterioration within the system due to normal wear and tear such as can deformation or weight loss from vibration and erosion. L-Seals are designed to provide these forces. Axial and radial mounting forces provided are derived from compression curves. The total mounting force provided by an L-Seal is essentially the aggregate of its radial (F_r) and axial (F_a) force contributions as described below.

$$F_T = F_a + F_r * \mu$$

Because an L-Seal cannot be mounted through the entire lateral surface of the substrate, its axial contribution needs to be maximized in order to meet its mounting requirement. Figure 3 indicates the typical axial force contribution of an L-Seal during the canning process.

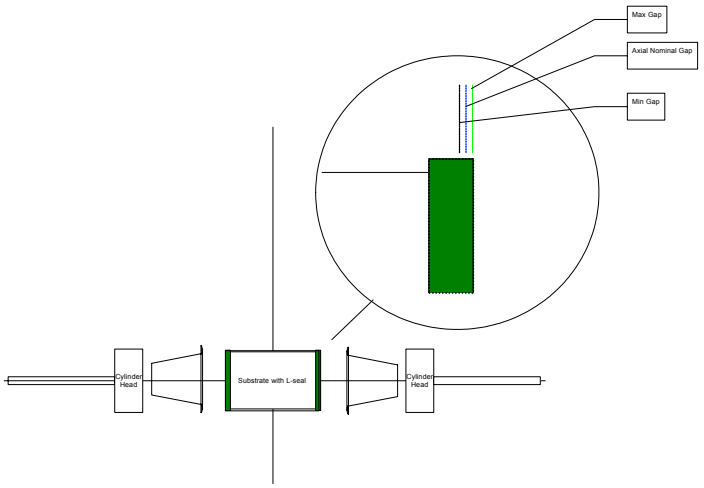

Figure 3: Axial Support in the Canning Process

L- SEAL DESIGN PROCESS

Figure 4 illustrates the sequential engineering steps in the L-Seal design process from conception to manufacturing.

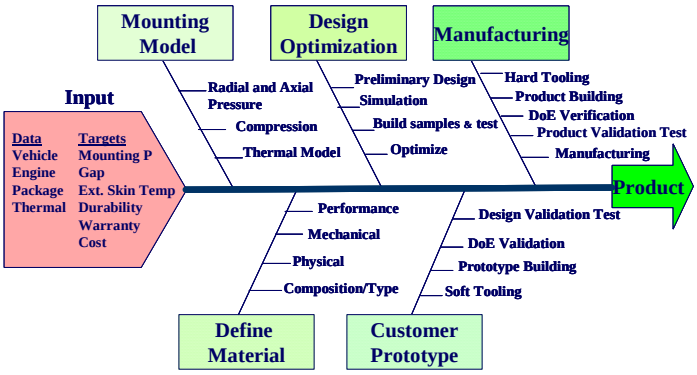

Figure 4: The L-Seal Development Process

The process starts with customer specified inputs such as vehicle information, engine characteristics, exhaust gas mass flow rate and a temperature histogram. Axial and radial forces, compression behavior and spring back curves are then modeled. Design optimization criteria and material selection are based on customer defined targets such as the radial

and axial gaps, initial and residual compressions, durability and weight. Prototypes are then produced and validated using optimized soft-tools. Next, Verification of Design of Experiment (DoE) and production validation (PV) tests on hard-tool products ultimately satisfy customer requirements.

COMPRESSION CHARACTERISTICS

An L-Seal's axial and radial compression characteristics are measured using a computer-controlled Instron or equivalent machine [15].

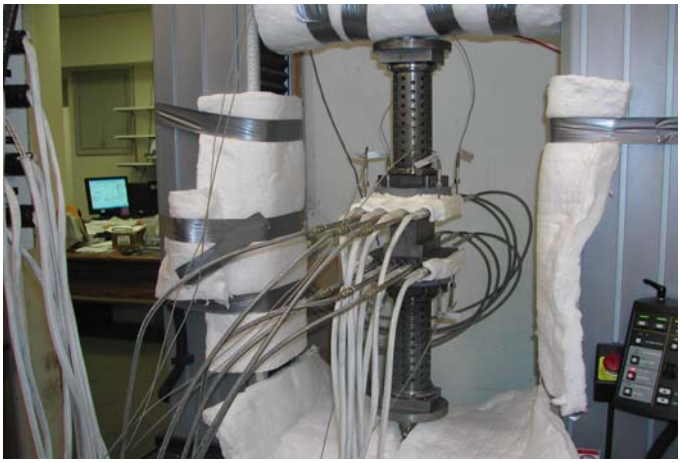

Figure 5: An Instron with a Heated Compression Assembly

Figures 6 and 7 indicate, respectively, radial and axial compression curves as a function of closing gap.

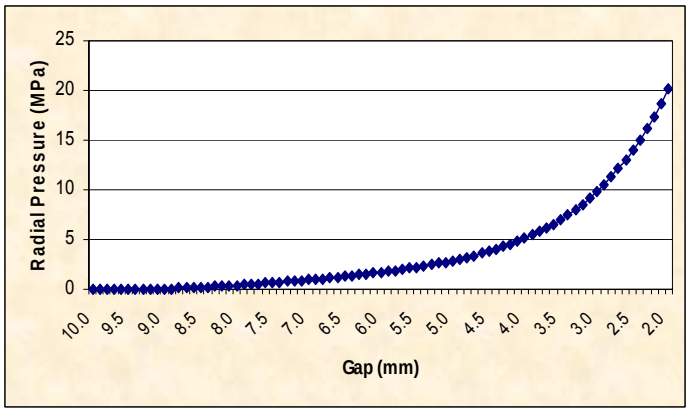

Figure 6. Radial Compression Curve

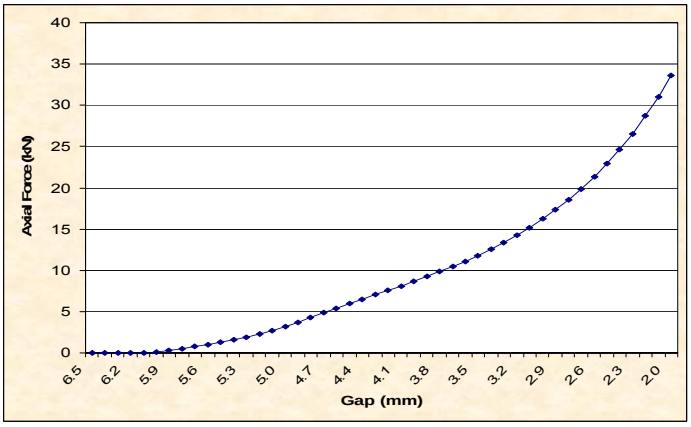

Figure 7. Axial Compression Curve

MATERIAL SELECTION CRITERIA

Material selection is base on the axial and radial compression requirements of the mounting system such as the desired overall length, leg length, radial gap, axial height and axial width. Variables such as wire material, geometry, density, wire mesh courses per inch, temper, surface profile and characteristics, needle count, number of strands and surface friction are manipulated to get the necessary axial and radial spring-back rates.

L-SEAL MATERIAL

Table 3 lists various materials used for L-Seals.

Material	A 286	SS 310
Chemical Composition		
Nominal Composition		
Chromium %	15	24 - 26
Aluminum %	0.2	0
Iron %	56 - 59	48 - 55
Nickel %	26	19 -22
Carbon %	0.08 max	0.25 max
Physical Characteristics		
Melting Point (°C)	1400	1400
Maximum operating temperature(°C)	982	900
Annealing Temperature(°C)	718 - 982	1040 - 1150
Density (g/cm^3)	7.91	7.75
Electric resistivity (µohm-m at 20 °C)	0.91	0.72
Coeff. Of thermal expansion (µm/m K)	9.17	15.9
Thermal Conductivity (W/m K)	17.8	14.2
Specific Heat (kJ/kg K)	0.42	0.50
Magnetic Permeability, H	1.01	1.00
Mechanical Properties		
Ultimate tensile strength (MPa)	620	515
Yield Strength (MPa)	275	205
Elongation at rupture (%)	40	40

Table 3: Material Attributes

L-Seals are generally made from A286, 310 SS or a combination of both. A286's high tensile and yield strengths and low thermal expansion coefficient provide a higher compressive force than 310. Combining the two, however, provides substantial control for honing in on specific spring-back rates. During heat-treatment A286 precipitate work-hardens, a phenomenon that provides nearly 20 % higher compression. Its resistance to corrosion and oxidation are also consistent with exhaust applications.

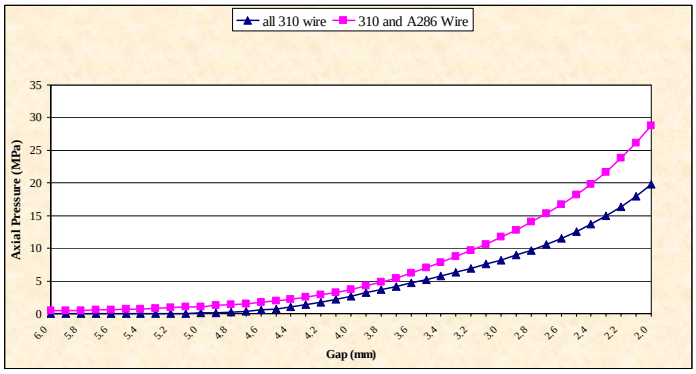

Figure 8: Comparative Axial Compression Curves of All 310 and 310/A286 L-Seal

L-SEAL DENSITY

As its weight increases, an L-Seal's compressive force increases as well.

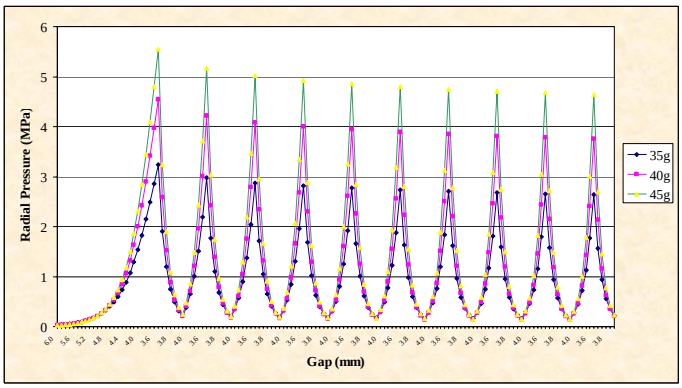

Figure 9: Compressive Force and Seal Weight

As noted in Figure 9, the 10-cycle compression curves range between 2.5 to 3.5 MPa on a 35 g seal and 4.7 to 5.5 MPa on a 45 g. The proportional increase in compressive force per unit of weight indicates the seal's dimensional consistency.

HEAT TREATMENT

As mentioned above, A286 precipitate work-hardens during heat-treatment. When combined with 310, the aggregate material can be tailored to meet spring-back rate requirements. Figures 10 and 11 illustrate this for both A286 and A286/310.

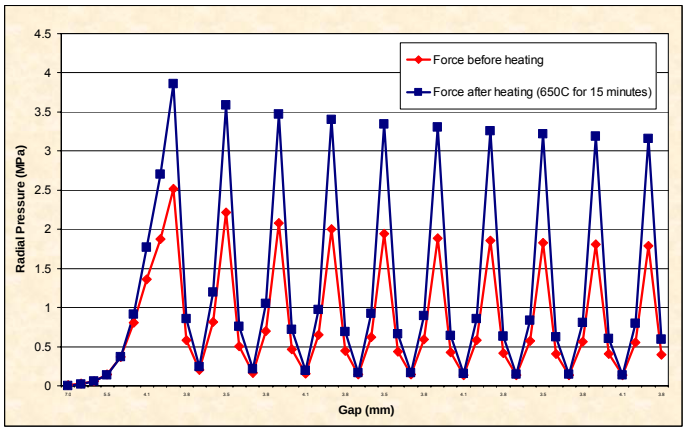

Figure 10: Radial Compression Test A286 Half Hard (HH) (10 Cycle)

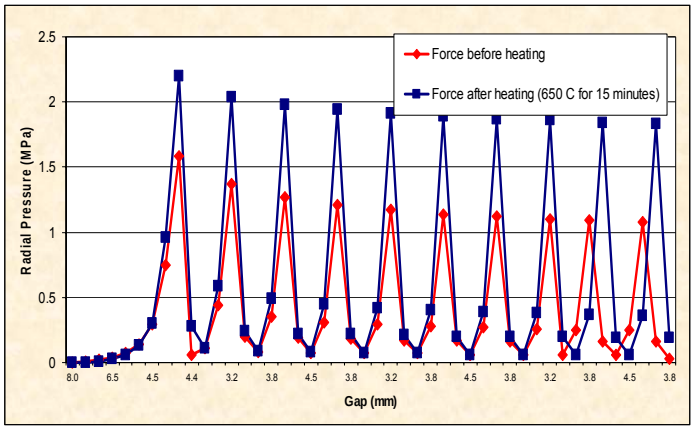

Figure 11. Radial Compression Test A286 HH + 310 (10 Cycle)

In both cases, radial pressure is measured before and after heat treatment. The cold compression force varied between 1.1 to 2.2 MPa. Heat-treating at 650 ^{o}C for 15 minutes produced a significant, 1.8 – 3.8 MPa, increase. L-Seals are generally made from heat-treated wire and further exposure to temperature did not yield any thermal loss (fig.12), thus indicating when A286 precipitation is complete.

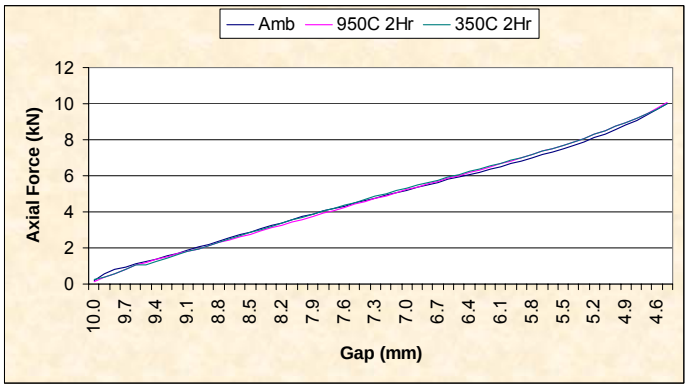

Figure 12: Axial Compressive Force of Heat treated L-Seal

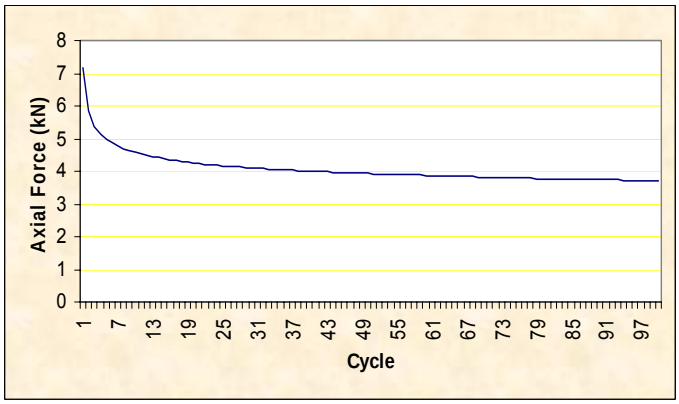

Figure 13: Axial Compression Test (100 Cycle)

10 and 100 cycle cold compression forces are measured to understand the spring back coefficient and to determine the material's residual force. Figure 13 gives the 100 cycle compression test of the A286/310 L-Seal and shows a stabilized force of about 50 % after repeated compression.

Figure 14 demonstrates the spring rate of said L-Seal at a specified gap.

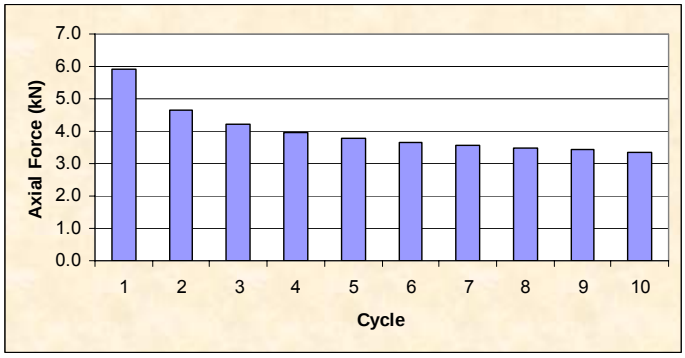

Figure 14. Axial Compression Force at defined Gap

Figure 15 indicates the loss of force during cycling at different gaps. As seen, the seal holds the same spring characteristics at these gaps, retaining its elastic function.

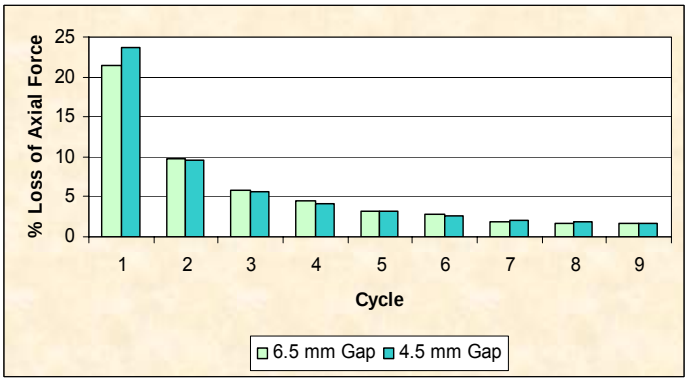

Figure 15. Loss of Force with Cycle

GAS PERMEABILITY

L-Seals are also expected to provide gas permeability. Figure 16 illustrates this function.

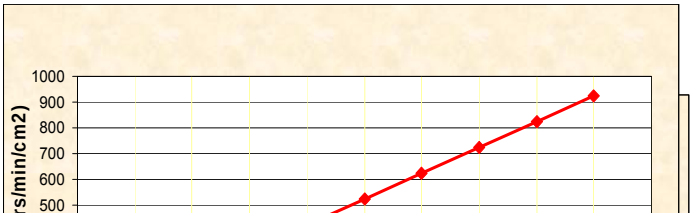

Figure 16: Gas Permeability Test

L-Seals can be modified to give very minimal differential pressures across the seal. Wire combinations such as half-flat/half-round or all round, can be used minimize the leak rate on the radial gap or provide more gas penetration, respectively.

PUSH OUT TEST

Figure 17 illustrates a standard push-out test. The force needed to dislodge substrate from its mounted position is measured and used to calculate the mounting pressure provided by the L-Seal. This is represented in Figure 18.

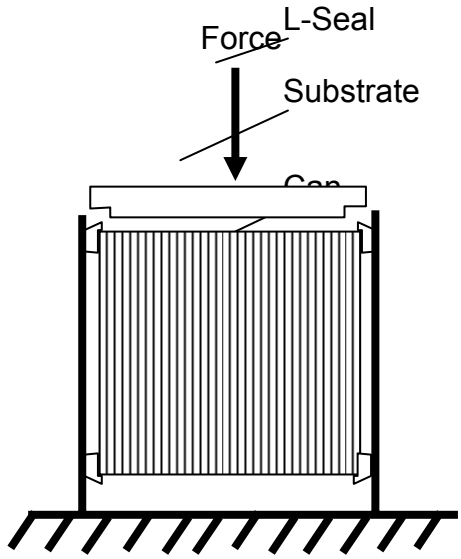

Figure 17: Representation of Push Out Test

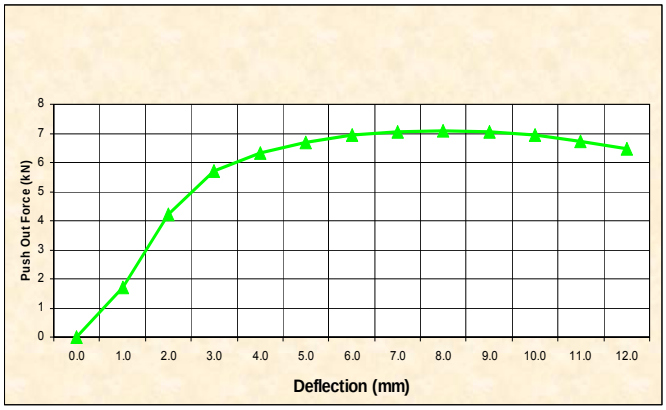

Figure 18: Push Out Force

PROCESS CAPABILITY

A manufacturing process capability study ensures there is dimensional consistency in production. Figure 19 shows one such study measuring the L-Seals' axial gap. The Cp and Cpk values indicate that the process is more than capable.

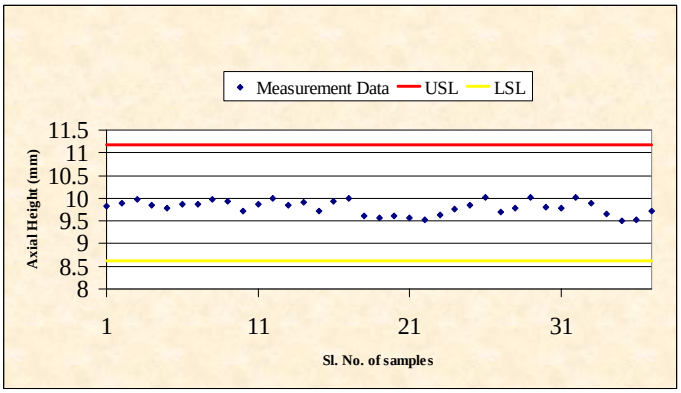

Figure19. Statistical Analysis of Axial Height

PRODUCT VALIDATION

DPF systems are validated to meet the thermal, mechanical and road-load conditions. Accelerated test conditions are established to ensure their lifetime survivability. Ambient and hot vibration, water quenches and oscillation load tests are usually performed to simulate these conditions. L-Seal mounted systems passed the required accelerated test conditions without field failures.

CONCLUSIONS

L-Seal mounting supports used in diesel particulate filters cushion the system by accommodating its components' linear tolerances and also provide the necessary axial and radial mounting forces.

- L-Seal axial and radial mounting forces are altered by type of material, surface characteristics, heat treatment and wire geometry.
- The proportional increase in compression force per unit weight during cycling shows dimensional consistency of the L-Seal.
- The compression characteristics of A286 tremendously increase (>20%) during heat treatment as precipitation and hardening occurs. Further heat treatment at DPF regeneration temperatures doesn't alter the compression characteristics.
- A A286/310 SS combination shows higher spring rate than all 310 SS.

- L-Seal compression force tends to stabilize during cycling, retaining a residual force of more than 50% of its initial value.

- Within the elastic limit of the L-Seal, the relative loss of force during cyclic compression as a function of closing gap is constant.

- Gas permeability of the L-Seal is altered using wire geometry.

- L-Seal provides combination of axial and radial mounting force for the DPF.

ACKNOWLEDGEMENTS

The authors acknowledge Steven Buckler, Jeff Buckler, Scott Mackenzie and Ray Scoboria, ACS Industries Inc. for their valuable assistance.

NOMENCLATURE

A_C	substrate frontal surface area
a	acceleration
F_A	axial force
F_a	axial force contribution of L-Seal
F_r	radial force contribution of L-Seal
F_T	total mounting force provided by L-Seal
F_B	backpressure force
F_I	inertial force
m_s	mass of the substrate
μ	friction coefficient
Δp	pressure drop across filter

REFERENCES

1. Johnson, T. V., “Diesel Emission Control – Last 12 Months in Review”, SAE 2000-01-2817.

2. Thalagavara, A. M., Johnson, J. H., Bagley, S. T., Shende, A. S., “The Effects of a Catalyzed Particulate Filter and Ultra Low Sulfur Fuel on Heavy Duty Diesel Engine Emissions”, 2005-01-0473.

3. Schenk, C., McDonald, J., Laroo, C., “High –Efficiency NOx and PM Exhaust Emission Control for Heavy-Duty On-Highway Diesel Engines- Part Two”, 2001-01-3619.

4. Katari, A., Syed, M., Sickels, M., Wahl, T., Rajadurai, S., “Effect off Aspect Ratio on Pressure Drop and Acoustics in Diesel Particulate Filters”, 2004-01-0695.

5. Harada, M., Ichikawa, S., Otsuka, A., Hattori, M., Hashimoto, S., “Durability Study on Si-SiC Material for DPF (3)”, 2005-01-0582.

6. Xinyum, Z., Zhi, N., Chunrun, Z., Yu, H., Shumin, L., “A Study on Trap Mechanism of Ceramic Foam”, 2000-01-2852.

7. Gulati, S. T., Leonhard, T., Roe, T. A., “Shear Strength of Cordierite Ceramic Catalyst Supports”, 2001-01-0935.

8. Ogunwumi, S. B., Tepesch, P.D., Chapman, T., Warren, C.J., Melscoet-Chauvel, I.M., Tennent, D.L., “Aluminium Titanate Compositions for Diesel Particulate Filters”, 2005-01-0583.

9. Heck, R.M., Farrauto, R.J., Gulati, R.J., “Catalytic Air Pollution Control – Commercial Technology”, Wiley, New York (2002).